J Appl Phycol (2008) 20:527–535
DOI 10.1007/s10811-007-9229-9

# Gel-forming structures and stages of red algal galactans of different sulfation levels

**Rando Tuvikene · Kalle Truus · Andres Kollist · Olga Volobujeva · Enn Mellikov · Tõnis Pehk**

Received: 21 April 2007 / Revised and accepted: 22 June 2007 / Published online: 8 August 2007


**Abstract** Sol-gel transition processes of algal galactans were studied using cryofixation method in combination with freeze-drying and scanning electron microscopy (SEM) techniques. The structures formed in successive stages of gelling process upon cooling were rapidly frozen at defined temperature points and viewed by SEM. It was established that in the case of both types of gelling galactans investigated, a fine honeycomb-like network exists for a wide range of solution temperatures. The formation and structure of this network depends on the structural type, gelling stage, and concentration of the galactan in solution. The honeycomb suprastructures exist also in carrageenan and agarose sols (at temperatures considerably exceeding the gelling temperatures). An additional helical network formed showed different behaviour in the case of carrageenan and agar-type polysaccharides. In the gel-formation process, tightening of the network takes place in both types of galactan gels; the honeycomb structures persist in carrageenan (furcellaran) but not in agarose gels.

**Keywords** Agarose · Furcellaran · Gel structure · Gelling process · Scanning electron microscopy

R. Tuvikene (✉) · K. Truus · A. Kollist
Department of Natural Sciences, Tallinn University,
Narva mnt 25,
10120 Tallinn, Estonia
e-mail: rtu@akvaarium.com

O. Volobujeva · E. Mellikov
Department of Materials Science,
Tallinn University of Technology,
Ehitajate tee 5,
19086 Tallinn, Estonia

T. Pehk
National Institute of Chemical Physics and Biophysics,
Akadeemia tee 23,
12618 Tallinn, Estonia

## Introduction

Red algal galactans are sulfated polysaccharides that usually have a linear backbone built up of alternating 3-linked β-D-galactopyranose and 4-linked α-galactopyranose residues. The β-galactose residues always belong to D-series, whereas the α-galactose residues are D in carrageenans and L in agars. A substantial part of α-galactose may exist in the form of a 3,6-anhydro derivative (Fig. 1). Various hydroxy groups may be substituted with ester sulfate, methyl groups, pyruvic acid acetal and sometimes with additional monosaccharide residues (Painter 1983; Usov 1998).

The most important characteristic of the red algal galactans is their gel-forming ability, i.e. the ability to form well-ordered spatial structures during cooling of their hot polymeric solution. The gelling ability gives the basis for the vital functions of red algae as well as for their use in food industry, microbiology, chromatography, electrophoresis, etc. (Therkelsen 1993). Gel formation in an aqueous solution is a complex process that depends on polysaccharide structure, polymer concentration and temperature, but also on the presence of co- and counter-ions (Morris et al. 1980; Meunier et al. 2001). Certain cations (typically $K^+$ for κ-carrageenan and furcellaran, $Ca^{2+}$ for ι-carrageenan) are found to induce conformational changes in the polymer with the initial coil-to-helix transition, which may be followed by subsequent aggregation of these helices to

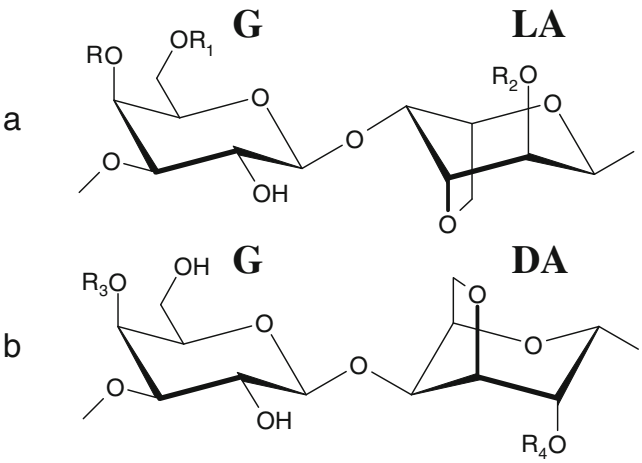


**Fig. 1** Disaccharide repeating units of **a** agars and **b** carrageenans. **a** *R* is H or $SO_3^-$, $R_1$ is H or Me or $SO_3^-$, $R_2$ is H or Me. **b** $R_3$ is $SO_3^-$, $R_4$ is H or $SO_3^-$ (κ- and ι-carrageenans, respectively). *G* is galactose and *A* is anhydrogalactose residue

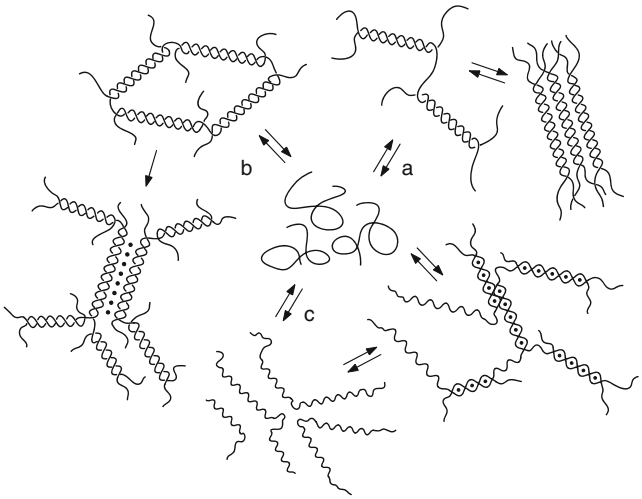


**Fig. 2** Models of gel formation: *a* double-helical model described by Anderson et al. (1969), *b* domain model proposed by Morris et al. (1980) and Robinson et al. (1980), and *c* nested, single-helix model proposed by Smidsrød and Grasdalen (1982). *Dots* indicate gel-promoting cations

form a gel (Rochas and Rinaudo 1984; Paoletti et al. 1985). The final gel structure is often determined by mutual interactions between conformational transition, molecular cross-linking and phase-separation processes.

It is generally accepted that gelation mechanisms for agars and carrageenans follow different pathways. The association processes of polymer chains have been extensively investigated beginning with well-known research by Rees (1969, 1972). From this time on, the studies on gelation of carrageenans and agars have mainly been concerned with the structure details of the junction zones of the gel-forming elements (Morris 1986; Piculell 1995), and some different models of gel formation have been proposed (Fig. 2). Anderson and co-workers (1969) suggested that the junctions are formed by intertwined double helices (double-helical model), whereas Morris et al. (1980) and Robinson et al. (1980) proposed that they are caused by cation-mediated aggregates of double helices (domain model). According to the model of Smidsrød and Grasdalen (1982), the junctions in the carrageenan networks are formed by cation-specific salt bridges between ordered chain segments (nested, single-helix model). The sequence of steps leading to gelation and the type of conformational transition (coil-helix or coil-double helix) are still a matter of debate.

While elementary processes of gel formation have been intensively studied during the last decades, the macroscopic gel level that directly determines rheological properties and is responsible for gel strength has been investigated to a much lesser extent. This kind of information has mainly been obtained from light-scattering measurements (Mangione et al. 2003), from hysteresis in optical rotation between cooling and heating curves (Borgström et al. 1996), from calorimetric and conductivity measurements during melting of aggregated structure (Watase et al. 1992) and from studies of turbidity and birefringence (Aymard et al. 2001). Various microscopy techniques have gained importance in such kinds of investigations, including scanning electron microscopy (SEM) (MacArtain et al. 2003), transmission electron microscopy (Stokke et al. 1993; Hermansson 1990), atomic force microscopy (Morris et al. 1997), scanning tunnelling microscopy (Lee et al. 1992) and confocal laser scanning microscopy (Ould Eleya et al. 2006; Bourriot et al. 1999). These methods often involve dehydrating samples after freezing structures at preferred states. To avoid shear-induced damage of supramolecular structures by formation and growth of ice crystals, microscopy techniques often involve several cryofixation methods, such as rapid freezing of samples in liquid propane or nitrogen at normal pressure or under vacuum (Dunstan et al. 2001). Also cryo-SEM in combination with pressure-shift freezing is extensively used for direct imaging of the undisturbed real-space gel structures at the micron scale (Fuchigami et al. 2006).

Numerous investigations have focused on the macroscopic gel structure of carrageenan blends with sugars, proteins or other industrial gums, such as agarose (Norziah et al. 2006), locust bean gum (Dunstan et al. 2001) and konjac gum (Medina-Torres et al. 2006). It has been reported that at a high level of co-solutes, galactans are severely water deficient, resulting in the occurrence of polysaccharide chains as a sparsely cross-linked network (Evageliou et al. 1998; Whittaker et al. 1997). Other studies suggest that, under such conditions, the polymeric chains are present as small, ordered gel particulates embedded within viscous solution (Richardson and Norton 1998;

Nickerson et al. 2004). Similar characteristics have also been found in the case of "pure" solutions, where the gelation processes can be affected by spinodal demixing of sol. San Biagio and co-workers (1996) found that at agarose concentrations below 2 wt%, spinodal demixing into mesoscopic polymer-rich and solvent-rich regions takes place before coil-double helix transition, whereas at higher concentrations gelation appears to proceed directly from the homogeneous solution state. Recently, mixing and pressure influences of rheological properties and macroscopic structure of galactan gels have also been studied (Ross et al. 2006).

It should be mentioned that despite the numerous papers published about gelling processes so far, the crucial stages of macroscopic gel formation have been studied insufficiently. Also there has been no systematic investigation published on galactan gel formation by cooling. In this work, an undersulfated κ-carrageenan from *Furcellaria lumbricalis*, furcellaran, was investigated in comparison with other carrageenan and agarose preparations. Rheology of furcellaran gels is somewhat different from that of the other carrageenans, showing more elastic properties and higher gel strength.

The aim of this paper is to elucidate principal stages in the gel formation process of red algal galactans (carrageenans and agars) at the macroscopic level. Special attention is given to the structural changes accompanying gradual cooling of sol and gel formation steps. The solidification process is monitored using cryofixation method in combination with freeze-drying and SEM.

## Experimental

### Galactan samples

Commercial agarose sample (standard EEO) was obtained from *Serva* (Heidelberg, Germany); κ-carrageenan preparation was purchased from *Fluka*. Furcellaran was isolated (Tuvikene et al. 2006) from the red alga *Furcellaria lumbricalis* (Kassari Bay, the Baltic Sea, Estonia) by hot alkaline extraction in 0.02 M KOH solution (at 100°C, 4 h) and precipitated by isopropanol (four-fold volume per extract). Agarose from *Ahnfeltia tobuchiensis* (Truus et al. 2006) (various lots of commercial production) was obtained from the pilot production plant of the Institute of Chemistry, Estonian Academy of Sciences.

According to the labelling, the *Serva* agarose sample contains 0.06% sulfur and less than 0.01% salts. Furcellaran was found to contain (w/w) 5.8% $K^+$, 0.07% $Na^+$, 1.2% $Ca^{2+}$ and 5.1% sulfur (bound to the matrix) as determined by ICP-OES method. This sample also contained a small amount of free salts.

### SEM measurements

Scanning electron microscopy was carried out on a high-resolution LEO Supra 35 electron microscope equipped with Röntec EDX XFlash 3001 detector and Thermo Noran Maxray ER Parallel Beam spectrometer. Samples were prepared by inserting preheated (≈95°C) stainless steel capillary tubes (inner diameter 2 mm, length 60 mm) into hot (≈95°C) 2% galactan solution (w/w) and allowing them to fill up. After gelling for 4 h at 20°C, the filled tubes were tightly closed. The prepared tubes were then heated on a water bath at 98°C for 30 min, followed by slow (0.5°C/min) cooling to 20°C. The samples removed from the thermostat during the cooling stage (at predetermined temperature) were rapidly frozen in liquid nitrogen at different stages of gel formation (from 90 to 20°C), cryofractured twice to produce small (5 mm in length) open-ended tubes filled with frozen gel, and freeze-dried under vacuum at −60°C. The formed cryogenic gel surfaces were sputter-coated with platinum of about 1 nm thickness using a Polaron High Resolution Sputter Coater SC7640 and examined under an acceleration voltage up to 1.7 kV.

The highly concentrated (16%, w/w) agarose gel specimen was investigated without any precaution; the gel was freeze-dried after solidification, treated with liquid nitrogen and cryofractured.

### Gel testing

For gel strength assessments, a simple gel tester equipped with a hemispherically tipped plunger (effective cross-section area 1 $cm^2$) was constructed. The gel strength measurements were done in triplicate for 1–2% gels (w/w) formed by dissolving dry galactan in hot water after gelling in an air thermostat at 20°C for 4 h. The cylindrical samples were 35 mm in diameter and 35 mm in height. The force needed to rupture the gel by the plunger was expressed in $g/cm^2$; a constant weight increase (350 g/min) was provided.

The melting temperature of the gel aged at 20°C for 4 hours was determined as the temperature at which a 4-mm glass bead fell down to the bottom of a screw-capped test tube (13×100 mm) during slow (0.5°C.$min^{-1}$) heating on a water bath. The tube was then cooled (0.5°C.$min^{-1}$) and turned horizontally every minute without removing it from the water bath. The gel-setting temperature was determined as the temperature at which the gel would no longer flow. All determinations of melting and gelling points were performed in duplicate.

### Spectrophotometrical measurements

Optical density measurements were made on a temperature-controlled Shimadzu UV-1601 spectrophotometer at 260 or

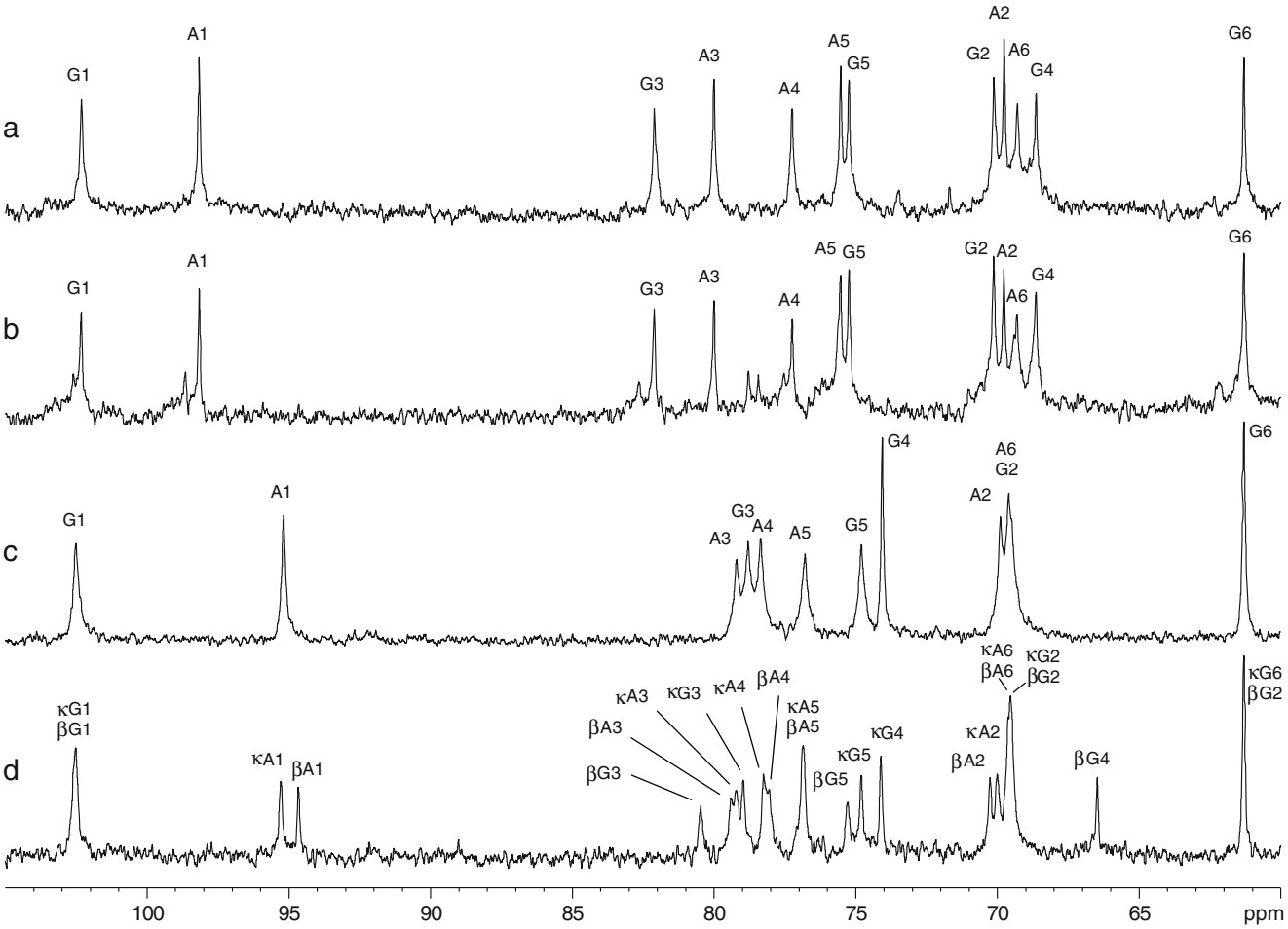


**Fig. 3** $^{13}$C-NMR spectra of galactan preparations. **a** Agarose *Serva*, recorded at 75°C, 6,700 transients. **b** Agarose from *A. tobuchiensis*, recorded at 75°C, 2,700 transients. **c** κ-Carrageenan *Fluka* purified by precipitation in isopropanol, recorded at 65°C, 5,700 transients. **d** Alkali-treated furcellaran, recorded at 85°C, 5,000 transients collected. β-Carrageenan signals correspond to the structure type in Fig. 1, part *b*, where $R_3$ and $R_4$ are H

400 nm against water as a blank. Hot (≈90°C) galactan solution was inserted into a 2-mm cuvette, sealed and thermostated in cuvette holder at 95°C for 5 min to allow sample equilibration. Thereafter, with continuous absorbance recording, the temperature was decreased slowly (0.5°C.min$^{-1}$) to 20°C, followed by isothermal hold for 50 min.

**Table 1** $^{13}$C-NMR chemical shifts (ppm) for basic signals of agar and carrageenan structures

| Galactan | Unit | $^{13}$C chemical shift | | | | | |
|---|---|---|---|---|---|---|---|
| | | C-1 | C-2 | C-3 | C-4 | C-5 | C-6 |
| Agarose | G | 102.3 | 70.1 | 82.1 | 68.6 | 75.2 | 61.3 |
| | LA | 98.2 | 69.8 | 80.0 | 77.2 | 75.5 | 69.3 |
| κ-Carrageenan | G | 102.5 | 69.6 | 78.8 | 74.1 | 74.8 | 61.3 |
| | DA | 95.2 | 69.9 | 79.2 | 78.4 | 76.8 | 69.6 |
| Furcellaran | κ G[a] | 102.5 | 69.5 | 79.0 | 74.1 | 74.8 | 61.3 |
| | κ DA[a] | 95.3 | 70.0 | 79.2 | 78.2 | 76.9 | 69.5 |
| | β G[b] | 102.5 | 69.5 | 80.5 | 66.5 | 75.3 | 61.3 |
| | β DA[b] | 94.7 | 70.3 | 79.4 | 78.0 | 76.9 | 69.5 |

[a] Corresponding units from κ-carrageenan
[b] Corresponding units from β-carrageenan

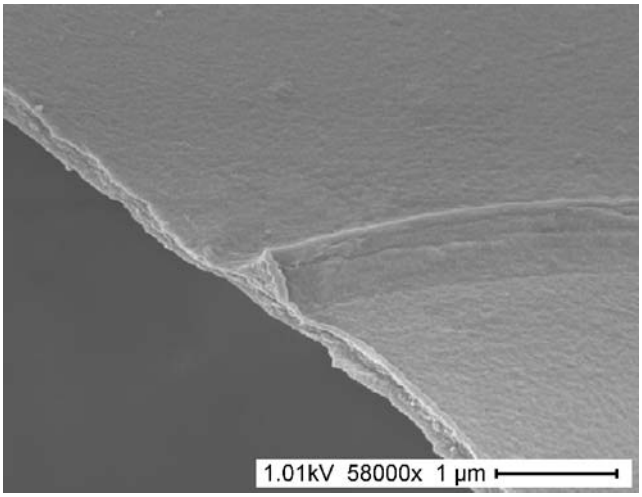


**Fig. 4** SEM image of the wall of honeycomb structure (freeze-dried 2% κ-carrageenan gel)

## NMR spectroscopy

Proton-decoupled $^{13}C$ nuclear magnetic resonance (NMR) spectroscopic analyses were carried out using a Bruker AMX-500 spectrometer. Spectra from 2% agarose or 4% carrageenan solution in $D_2O$ (w/w) were obtained at 65–85°C, and about 2,700–6,700 transients were collected before the Fourier transform. Chemical shifts were converted to a tetramethyl silane scale on the basis of the C6 signal from the galactose subunit with a constant value (61.3 ppm) in these galactans (Usov and Shashkov 1985).

## Results and discussion

### Molecular structure

$^{13}C$-NMR spectra of four galactans investigated are presented in Fig. 3. The spectra allow (Usov et al. 1980) different galactan types (agaroses, carrageenans) to be distinguised on the basis of absolute configuration of the 1,4-linked anhydrogalactose ring. Undersulfation in furcellaran molecule causes additional resonance signals in $^{13}C$-NMR spectrum (compared to commercial κ-carrageenan preparations) corresponding to carbons of non-sulfated β-carrageenan units (Knutsen and Grasdalen 1987). The values of chemical shifts for basic carbon signals of the galactans investigated are presented in Table 1. The values are in accordance with literature data (Van de Velde et al. 2002). The shift values of two investigated agaroses of different origin coincide, which is typical of commercial high-quality agaroses (Truus et al. 2006). Thus the structural type and characteristics of the galactans to be studied were established.

### Scanning electron microscopy

To avoid structural damages to shock-sensitive SEM preparations during the rapid cooling process, galactan solutions were tightly enclosed in tubes (except in the case of very high concentrations, for which the mechanical strength of the sample is high). Material and dimensions of

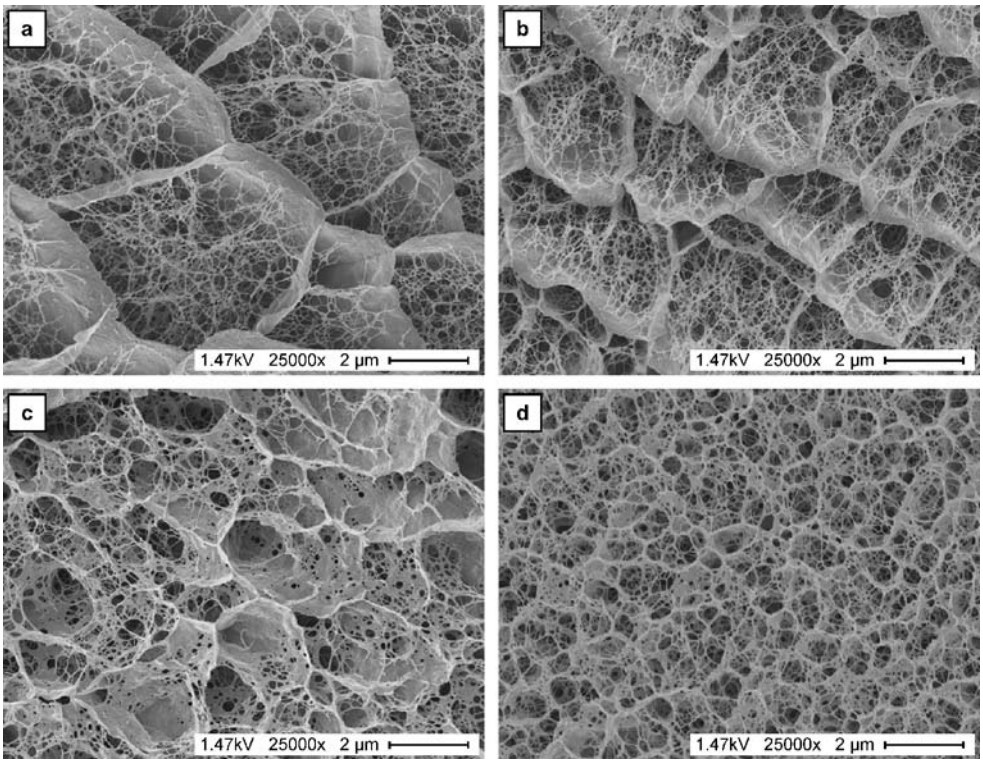


**Fig. 5** SEM images of 2% agarose gel network structures at **a** 70°C, **b** 40°C, **c** 30°C and **d** 20°C

the tubes were chosen to guarantee the rapid freezing process and to handle samples without loss of the frozen state for any moment. Subsequent use of cryo-fracture and freeze-drying techniques were calculated to preserve the real structures corresponding to the desired gel-forming stage as well as to preserve the surface with an appropriate texture for SEM investigations. Generally, it has been accepted for some decades that ultrafast freezing techniques allow for the avoidance of distortions and defects in specimens even to the nanometer scale (Echlin 1978; Robards 1991). Also it was concluded from the gradual elaboration of the preparation technique and from the quality of the images achieved that any considerable damage to the specimens or any corresponding artefacts before direct SEM investigations had been avoided. From the investigation of the gelling processes based on SEM images, the following observations were made.

We observed novel precursor structures already at quite high (70°C) temperatures, significantly exceeding the macroscopic gelling temperature (which is the final result of numerous gel-forming microprocesses). Characteristic honeycomb structures appeared in agarose and furcellaran sols of low concentration already at high temperatures considerably exceeding the gelling point. The walls of the honeycomb structures were rather thin (about 100 nm in carrageenan gels, Fig. 4) for conventional SEM investigations. The quality of the images and high resolution are due to the new-generation microscope used. Similar supramolecular structures have been described in the case of mixed gels (Dunstan et al. 2001).

Compared to furcellaran, the structural units of the honeycomb network (cells) in agarose were considerably smaller, for example, at the gelling stage of 20°C, nearly a 10-fold difference existed. In the case of agarose gels, there

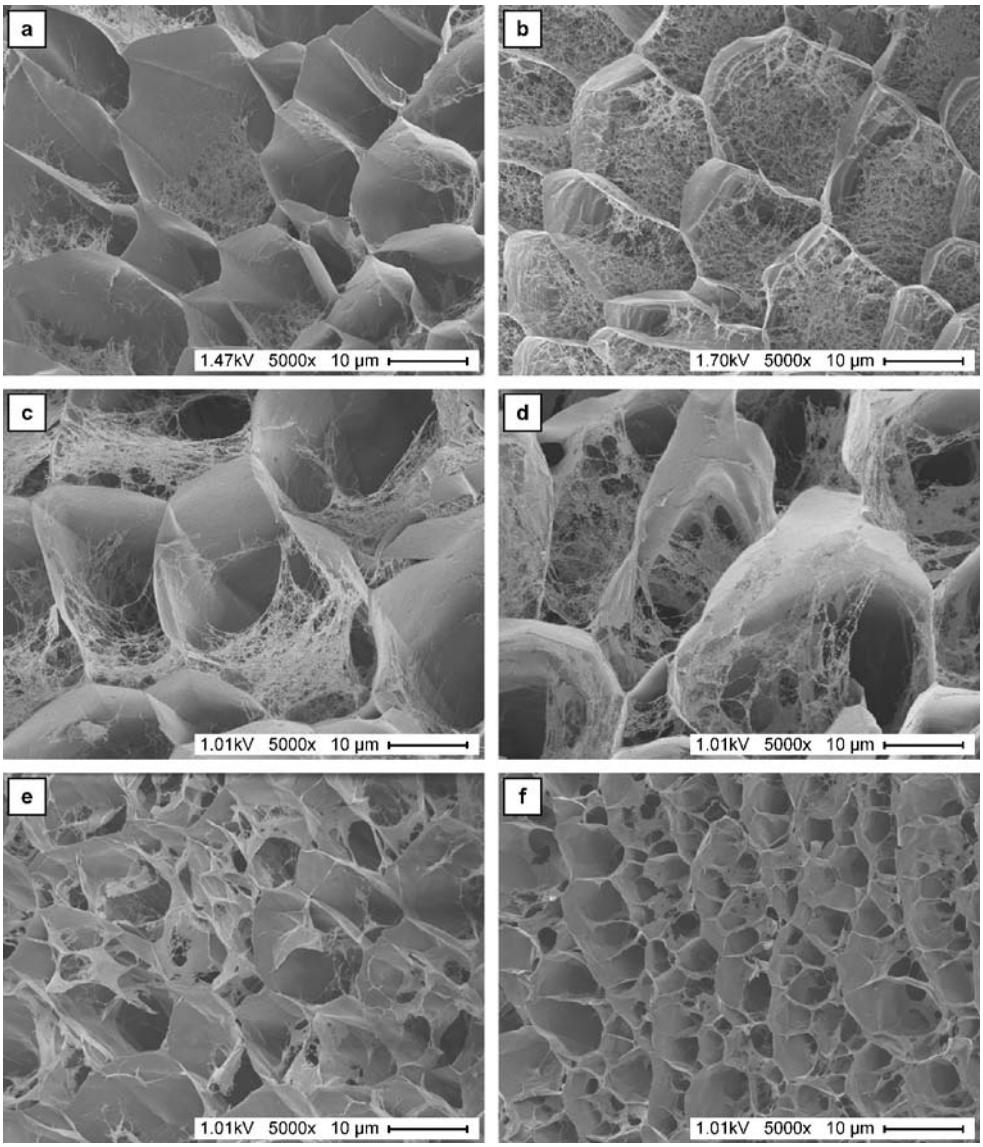


**Fig. 6** SEM images of 2% furcellaran gel network structures at **a** 70°C, **b** 50°C, **c** 40°C, **d** 35°C, **e** 30°C and **f** 20°C

was a high dependence of cell diameter on the temperature of the gelation stage; furcellaran gels did not show such a strong correlation (not shown).

The honeycomb structures are filled with tight polysaccharide networks, detailed peculiarities of which depend on the gelling stage or temperature. In the case of agarose gels, the quota of reticulated (helical) structures increased through the cooling process during which honeycomb structures disappeared. An opposite tendency was observed in furcellaran gels, where the honeycomb pattern persisted also at low temperatures but the thin network disappeared (compare Figs. 5 and 6). This was the main qualitative difference in the gel-formation process between agar- and carrageenan-type polysaccharides. Also it was remarkable that the thickening of honeycomb structures in furcellaran gel occurred due to decreasing proportion of thin polysaccharide network; in this case, conversion of the network to honeycomb structure takes place (Fig. 6c,e).

The fact that honeycomb structures were able to change their shape and disappear (under the same sample preparation conditions) assures that there no substantial artefacts were being created. Also, the specimens did not show any cleavage or other damage. On the other hand, these honeycombs are not static walls (because of their liquid state) but rather potential and dynamic precursor structures reflecting the hidden collectivity tendencies of this type of macromolecules.

The greatest changes in gel structure during the cooling process took place considerably below the gelling temperature of the galactan sol. This is related to the thickening of structures, which caused a high increase in optical density (see Figs. 5, 6, 7). At that, some characteristic honeycomb structures existed in both types of galactan gels observed. The walls of honeycombs are quite specific structural units. These seem to be thin, even films without any noticeable structure. This seemingly plain structure is conditioned by the resolution limits of SEM techniques at the present time. As it appears from the images (Fig. 6c), wall formation is related to helical structure. However, it can be seen that the walls were double-layered (Fig. 4); compared to carrageenan gels, wall thickness was much less in agarose gels.

Depending on the structural characteristics of agarose, the macroscopic gel structure can vary considerably even in the case of preparations gelled under the same conditions; samples of lower gel strength (Table 2) showed sparser structural patterns (Fig. 8a,b). It seems to be evident that the course of gel formation as well as the final gel structure depends on numerous characteristics such as galactan structure, sol concentration, and gelling conditions. Also the cell size was highly dependent on galactan concentration (Fig. 8b,c). Gels of very high concentrations were of markedly different structure (Fig. 8d).

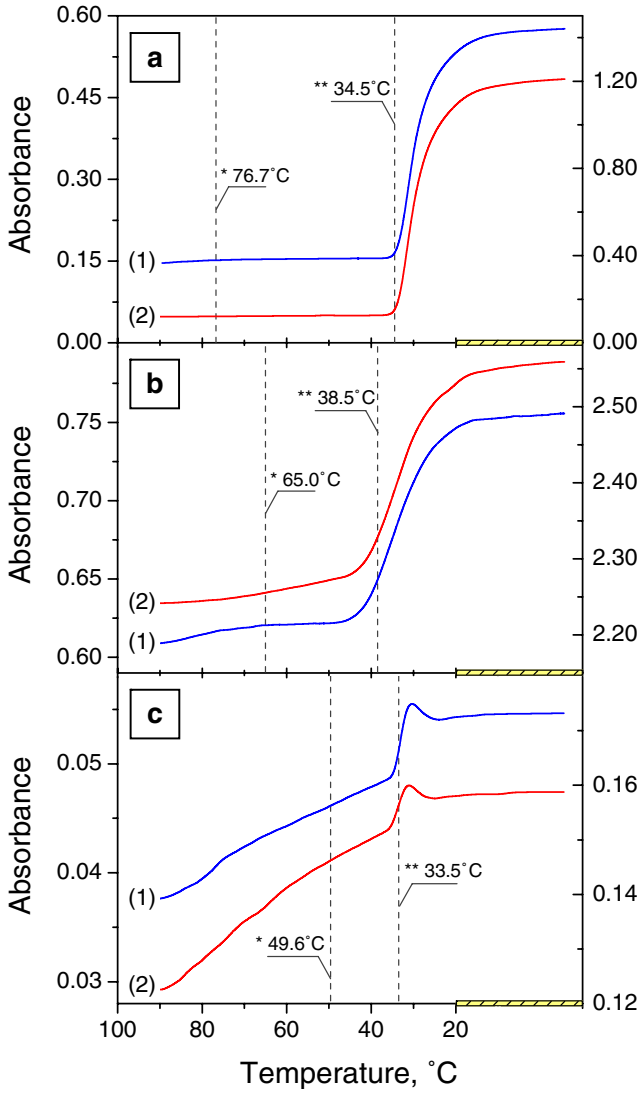


**Fig. 7** Gelling profiles for galactan solutions (2%, w/w) at cooling rate of 0.5°C/min. Absorbance measured at 260 nm (*right scale*) and 400 nm (*left scale*) in 2-mm cuvette. *Two asterisks* indicate gelling temperature, *one asterisk* indicates gel melting temperature, (▨) indicates the isothermal region (20°C). **a** Agarose from *Ahnfeltia tobuchiensis*, **b** furcellaran, **c** κ-carrageenan (*Fluka*)

## Spectrophotometrical and rheological investigations

The formation and stabilization of tightly packed structures is related to an increase in optical density (Fig. 7). For agarose gels this change is sharper and expresses well their gelling temperature. Although in the case of furcellaran, the tightening of large-cell honeycomb patterns occurs mainly in the gel state, the increase in optical density of their sols takes place well before reaching the gelling temperature.

The commercial κ-carrageenan preparation was evidently somewhat degraded (with a weak gelling ability at low concentration, Table 2) and contained impurities, probably

**Table 2** Gel strength at various galactan concentrations

| Galactan | Gel strength (g/cm$^2$) | | |
|---|---|---|---|
| | 1% | 1.5% | 2% |
| Agarose *Serva* | 665 | 1,360 | 1,850 |
| Agarose from *A. tobuchiensis* | 260 | 500 | 725 |
| κ-Carrageenan *Fluka* | 15 | 380 | 1,350 |
| Alkali-treated furcellaran[a] | 445 | 800 | 1,110 |

[a] Extracted in 0.02 M KOH solution (at 100°C, 4 h)

some low-molecular carbohydrates, as confirmed by NMR spectra (not shown). The impurities affected the whole gelling process (Fig. 7c), and the preparations made were unsuitable for SEM investigations. In contrast, good gelling properties of furcellaran permitted preparation of high-quality SEM specimens.

## Conclusions

In the gelling process of polysaccharides containing 3,6-anhydrogalactose, a fine honeycomb-like network participates as a "hidden" precursor structure. This network exists in galactan solutions at significantly higher temperatures than those of rheological changes related to gel formation.

Although the honeycomb structures exist in carrageenan as well as in agarose sols and gels, the behaviour of this fine network in gelling processes depends on the structural type of the galactan, i.e. on the configuration of the anhydrogalactose ring (AGR).

Carrageenan-type galactans (containing AGR of D-configuration) form gels mainly by tightening of the honeycomb network; other structures disappear in the course of the final gel formation. Correspondingly, carrageenan gels consist of a very fine network and are highly elastic. In contrast, agar-type galactans (containing L-AGR) gradually lose their honeycomb structure in the course of gel formation. Therefore the final structure of agar/agarose gels is built up of a more tight and homogeneous network, resulting in brittle, strong gels of high light absorbance.

The gel-forming process is highly sensitive to structural and compositional characteristics of galactans; gels of high galactan concentration may be of essentially different structure than those of low polysaccharide content.

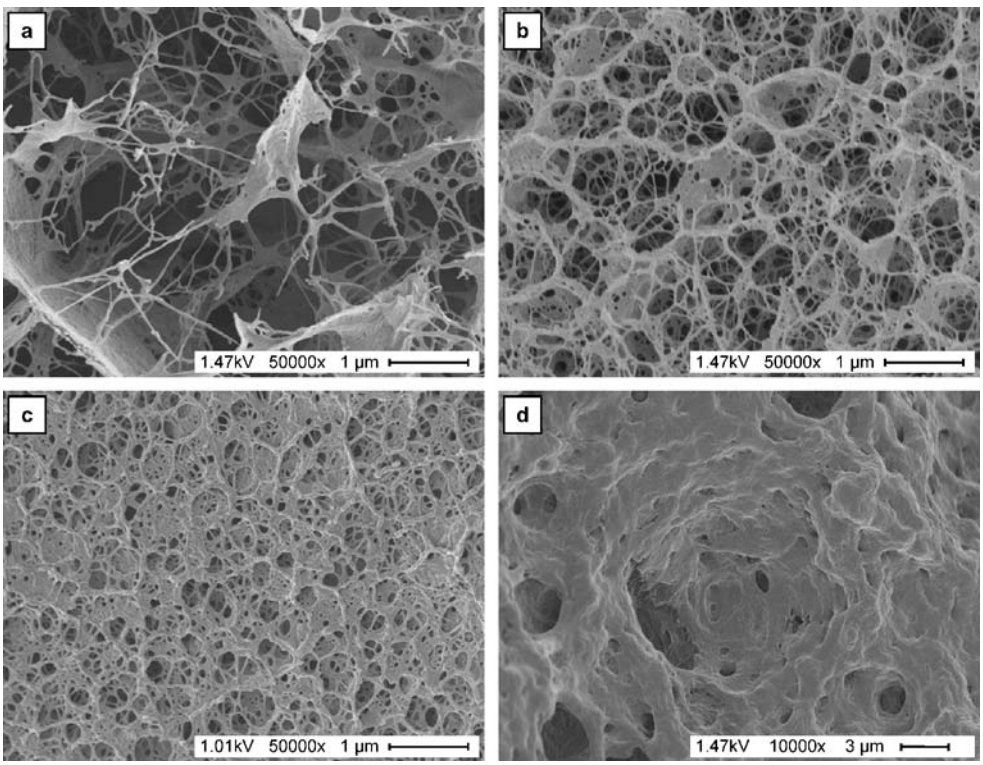


**Fig. 8** SEM images of gel network structures at 20°C of **a** 2% agarose from *Ahnfeltia tobuchiensis*, and **b** 2%, **c** 6% and **d** 16% agarose (*Serva*)

## References


Anderson NS, Campbell JW, Harding MM, Rees DA, Samuel JWB (1969) X-ray diffraction studies of polysaccharide sulfates: double helix model for κ- and ι-carrageenans. J Mol Biol 45:85–99

Aymard P, Martin DR, Plucknett K, Foster TJ, Clark AH, Norton IT (2001) Influence of thermal history on the structural and mechanical properties of agarose gels. Biopolymers 59:131–144

Borgström J, Piculell L, Viebke C, Talmon Y (1996) On the structure of aggregated kappa-carrageenan helices. A study by cryo-TEM, optical rotation and viscometry. Int J Biol Macromol 18:223–229

Bourriot S, Garnier C, Doublier J-L (1999) Micellar casein/kappa-carrageenan mixtures. 1. Phase separation and ultrastructure. Carbohydr Polym 40:145–157

Dunstan DE, Chen Y, Liao M-L, Salvatore R, Boger DV, Prica M (2001) Structure and rheology of the kappa-carrageenan/locust bean gum gels. Food Hydrocolloids 15:475–484

Echlin P (1978) Low-temperature biological scanning electron microscopy. In: Koehler KJ (ed) Advanced techniques in biological electron microscopy II. Springer, Berlin, pp 89–122

Evageliou V, Kasapis S, Hember MWN (1998) Vitrification of κ-carrageenan in the presence of high levels of glucose syrup. Polymer 39:3909–3917

Fuchigami M, Teramoto A, Jibu Y (2006) Texture and structure of pressure-shift-frozen agar gel with high visco-elasticity. Food Hydrocolloids 20:160–169

Hermansson A-M (1990) Structure and rheological properties of kappa-carrageenan gels. In: Burchard W, Ross-Murphy SB (eds) Physical networks: polymers and gels. Elsevier, London, pp 271–282

Knutsen SH, Grasdalen H (1987) Characterization of water-extractable polysaccharides from Norwegian *Furcellaria lumbricalis* (Huds.) Lamour. (Gigartinales, Rhodophyceae) by IR and NMR spectroscopy. Bot Mar 30:497–505

Lee I, Atkins EDT, Miles MJ (1992) Visualisation of the algal polysaccharide carrageenan by scanning tunnelling microscopy. Ultramicroscopy 42–44:1107–1112

MacArtain P, Jacquier JC, Dawson KA (2003) Physical characteristics of calcium induced κ-carrageenan networks. Carbohydr Polym 53:395–400

Mangione MR, Giacomazza D, Bulone D, Martorana V, San Biagio PL (2003) Thermoreversible gelation of kappa-carrageenan: relation between conformational transition and aggregation. Biophys Chem 104:95–105

Medina-Torres L, Brito-De La Fuente E, Gómez-Aldapa CA, Aragon-Piña A, Toro-Vazquez JF (2006) Structural characteristics of gels formed by mixtures of carrageenan and mucilage gum from *Opuntia ficus indica*. Carbohydr Polym 63:299–309

Meunier V, Nicolai T, Durand D (2001) Structure of aggregating κ-carrageenan fractions studied by light scattering. Int J Biol Macromol 28:157–165

Morris ER, Rees DA, Robinson G (1980) Cation-specific aggregation of carrageenan helices: domain model of polymer gel structure. J Mol Biol 138:349–362

Morris VJ (1986) Gelation of polysaccharides. In: Mitchell JR, Ledward DA (eds) Functional properties of food macromolecules. Elsevier, London, pp 121–170

Morris VJ, Gunning AP, Kirby AR, Round A, Waldron K, Ng A (1997) Atomic force microscopy of plant cell walls, plant cell wall polysaccharides and gels. Int J Biol Macromol 21:61–66

Nickerson MT, Paulson AT, Speers RA (2004) Time-temperature studies of gellan polysaccharide gelation in the presence of low, intermediate and high levels of co-solutes. Food Hydrocolloids 18:783–794

Norziah MH, Foo SL, Karim AA (2006) Rheological studies on mixtures of agar (*Gracilaria changii*) and κ-carrageenan. Food Hydrocolloids 20:204–217

Ould Eleya MM, Leng XJ, Turgeon SL (2006) Shear effects on the rheology of β-lactoglobulin/β-carrageenan mixed gels. Food Hydrocolloids 20:946–951

Painter TJ (1983) Algal polysaccharides. In: Aspinall GO (ed) The polysaccharides, vol. 2. Academic, New York, pp 195–285

Paoletti S, Delben F, Cesàro A, Grasdalen H (1985) Conformational transition of κ-carrageenan in aqueous solution. Macromolecules 18:1834–1841

Piculell L (1995) Gelling carrageenans. In: Stephen AM (ed) Food polysaccharides and their applications. Marcel Dekker, New York, pp 205–244

Rees DA (1969) Structure, conformation, and mechanism in the formation of polysaccharide gels and networks. Adv Carbohydr Chem Biochem 24:267–332

Rees DA (1972) Polysaccharide gels. A molecular view. Chem Ind (London) 19:630–636

Richardson RH, Norton IT (1998) Gelation behavior of concentrated locust bean gum solutions. Macromolecules 31:1575–1583

Robards AW (1991) Rapid-freezing methods and their applications. In: Hall JL, Hawks C (eds) Electron microscopy of plant cells. Academic, London, pp 257–312

Robinson G, Morris ER, Rees DA (1980) Role of double helices in carrageenan gelation: the domain model. J Chem Soc Chem Commun 1980:152–153

Rochas C, Rinaudo M (1984) Mechanism of gel formation in κ-carrageenan. Biopolymers 23:735–745

Ross KA, Pyrak-Nolte LJ, Campanella OH (2006) The effect of mixing conditions on the material properties of an agar gel. Food Hydrocolloids 20:79–87

San Biagio PL, Bulone D, Emanuele A, Palma-Vittorelli MB, Palma MU (1996) Spontaneous symmetry-breaking pathways: time-resolved study of agarose gelation. Food Hydrocolloids 10:91–97

Smidsrød O, Grasdalen H (1982) Some physical properties of carrageenan in solution and gel state. Carbohydr Polym 2:270–272

Stokke BT, Elgsaeter A, Kitamura S (1993) Macrocyclization of polysaccharides visualized by electron microscopy. Int J Biol Macromol 15:63–68

Therkelsen GH (1993) Carrageenan. In: Whistler RL, BeMiller JN (eds) Industrial gums: polysaccharides and their derivatives, 3rd ed. Academic, San Diego, pp 145–180

Truus K, Tuvikene R, Vaher M, Kailas T, Toomik P, Pehk T (2006) Structural and compositional characteristics of gelling galactan from the red alga *Ahnfeltia tobuchiensis* (Ahnfeltiales, the Sea of Japan). Carbohydr Polym 63:130–135

Tuvikene R, Truus K, Vaher M, Kailas T, Martin G, Kersen P (2006) Extraction and quantification of hybrid carrageenans from the biomass of the red algae *Furcellaria lumbricalis* and *Coccotylus truncatus*. Proc Estonian Acad Sci Chem 55:40–53

Usov AI (1998) Structural analysis of red seaweed galactans of agar and carrageenan groups. Food Hydrocolloids 12:301–308

Usov AI, Shashkov AS (1985) Polysaccharides of algae. XXIV. Detection of iota-carrageenan in *Phyllophora brodiaei* (Turn.) J. Ag. (Rhodophyta) using $^{13}$C-NMR spectroscopy. Bot Mar 28:367–373

Usov AI, Yarotsky SV, Shashkov AS (1980) $^{13}$C NMR spectroscopy of red algal galactans. Biopolymers 19:977–990

Van de Velde F, Knutsen SH, Usov AI, Rollema HS, Cerezo AS (2002) $^{1}$H and $^{13}$C high resolution NMR spectroscopy of carrageenans: applications in research and industry. Trends Food Sci Technol 13:73–92

Watase M, Kohyama K, Nishinari K (1992) Effects of sugars and polyols on the gel-sol transition of agarose by differential scanning calorimetry. Thermochim Acta 206:163–173

Whittaker LE, Al-Ruqaie IM, Kasapis S, Richardson RK (1997) Development of composite structures in the gellan polysaccharide/sugar system. Carbohydr Polym 33:39–46